

Supporting Information

A New Class of Battery-free, Mechanically Powered, Piezoelectric $\text{Ca}_5\text{Ga}_6\text{O}_{14}:\text{Tb}^{3+}$ Phosphor with Self-recoverable Luminescence

Tao Hu^{a*}, Yan Gao^a, Bo Wang^a, Ting Yu^a, Dawei Wen^a, Yao Cheng^{b,c*}, Qingguang Zeng^a

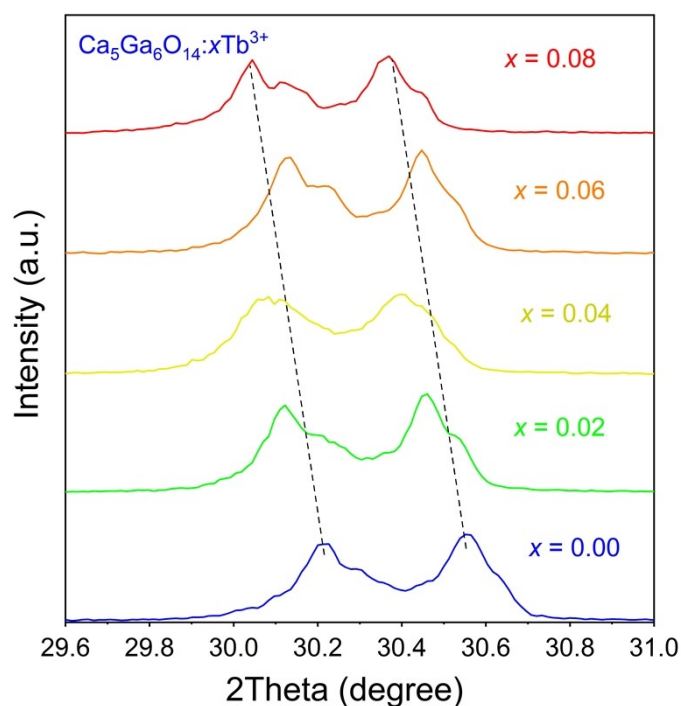


Figure S1. Enlarged view of the XRD diffraction peaks in the 2θ range of 29.6–31.0 degree.

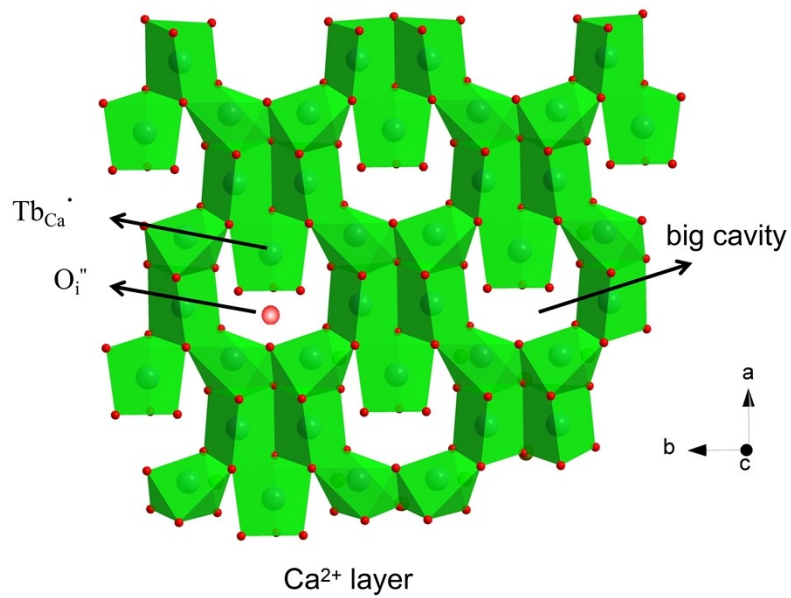


Figure S2. Monolayer crystal structure viewing along *c*-axis.

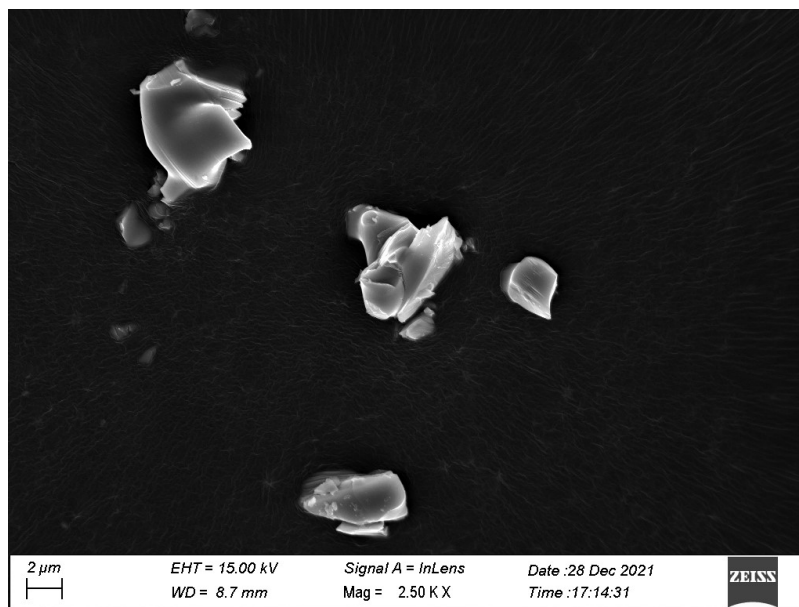


Figure S3. SEM image of the phosphor

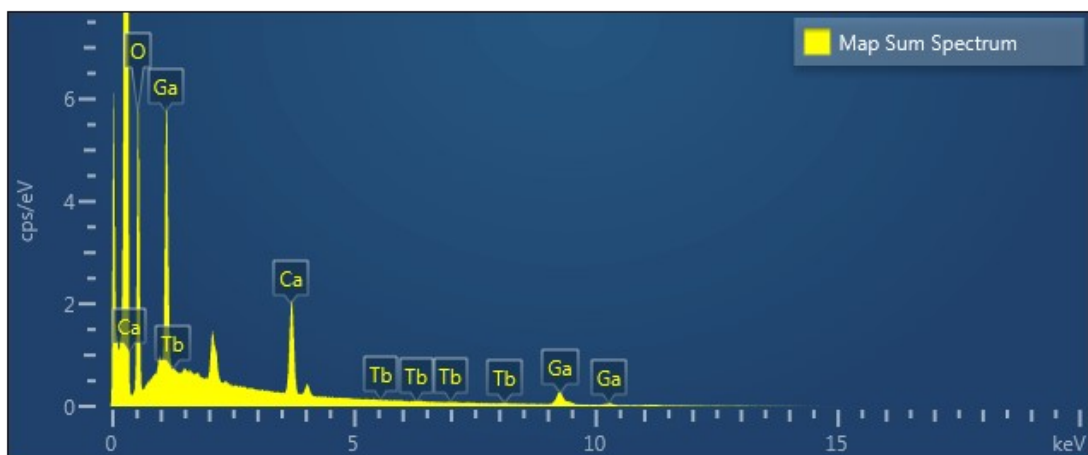


Figure S4. EDS analysis on the phosphor

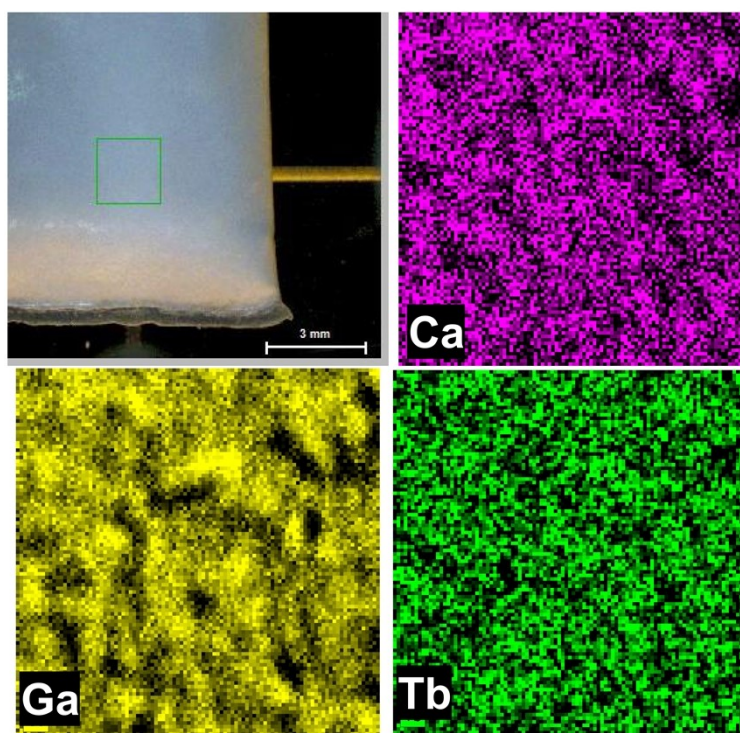


Figure S5. The distribution of Ca, Ga, and Tb³⁺ ions measured by XRF

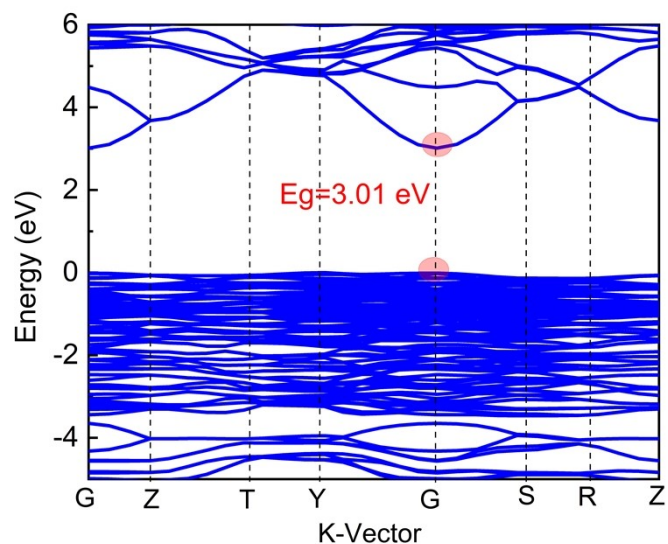


Figure S6. The calculated energy band structure of $\text{Ca}_5\text{Ga}_6\text{O}_{14}$ host.

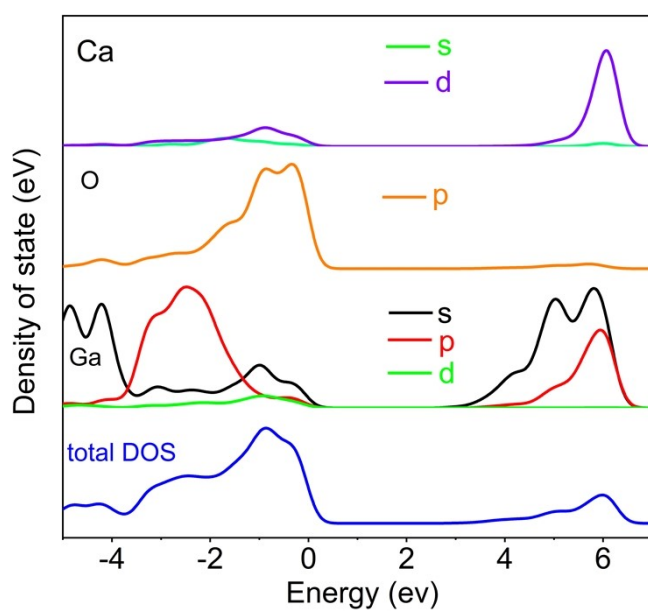


Figure S7. The partial (of Ca, Ga and O atom) and the total density state density of states for $\text{Ca}_5\text{Ga}_6\text{O}_{14}$ host.

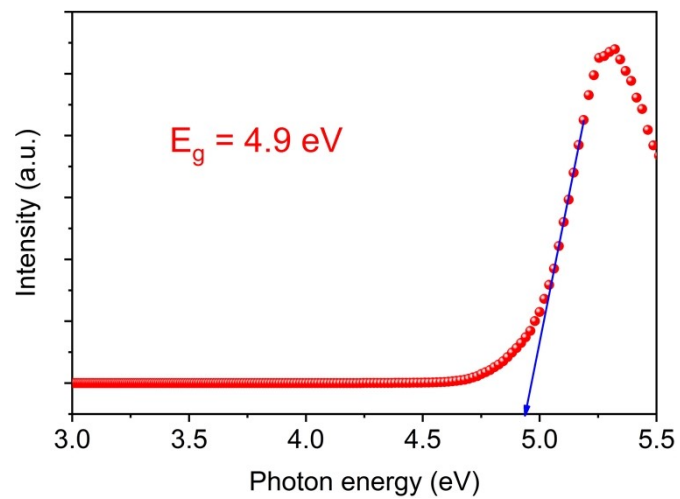


Figure S8. The calculated bandgap for $\text{Ca}_5\text{Ga}_6\text{O}_{14}$

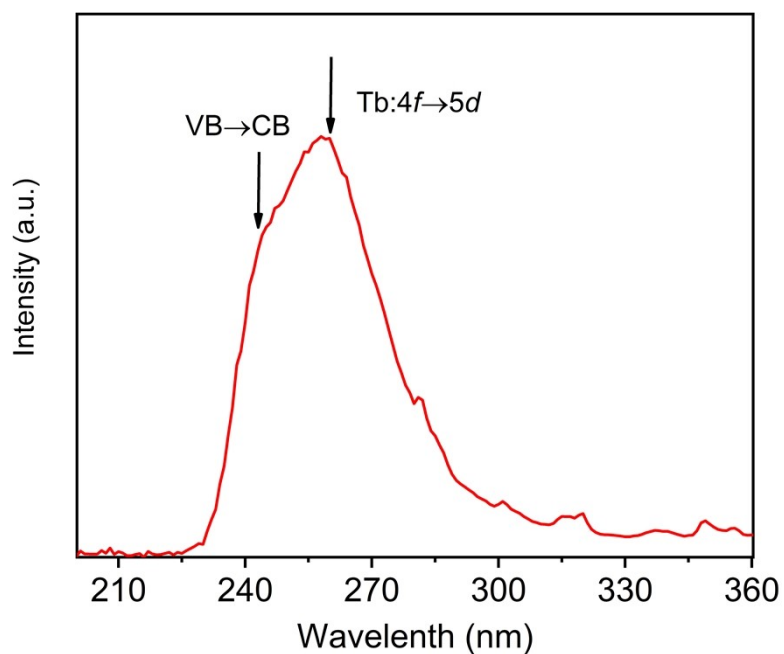


Figure S9. The PLE spectra of $\text{Ca}_5\text{Ga}_6\text{O}_{14}:\text{Tb}^{3+}$ phosphor by monitoring at 543 nm emission

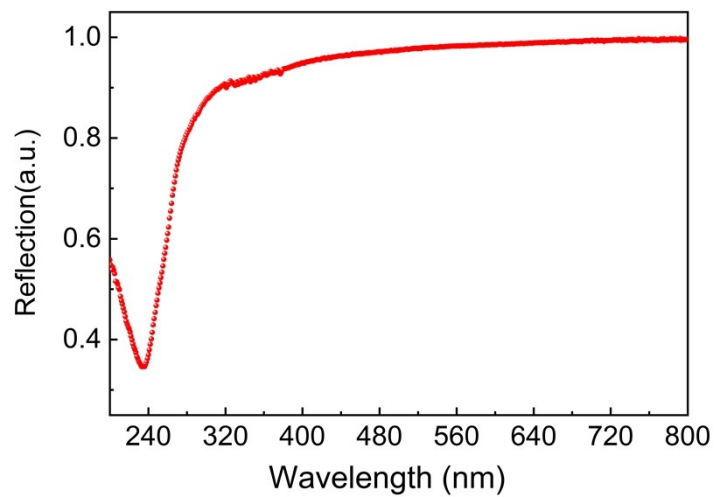


Figure S10. The absorption spectra of $\text{Ca}_5\text{Ga}_6\text{O}_{14}:\text{Tb}^{3+}$ phosphor showing a strong absorption dip at 240 nm.

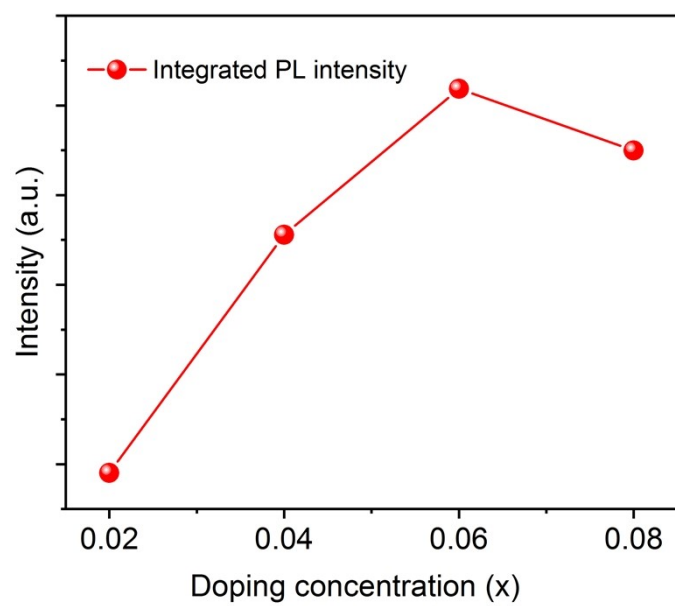


Figure S11. Integrated PL intensity of $\text{Ca}_5\text{Ga}_6\text{O}_{14}:\text{xTb}^{3+}$ phosphor

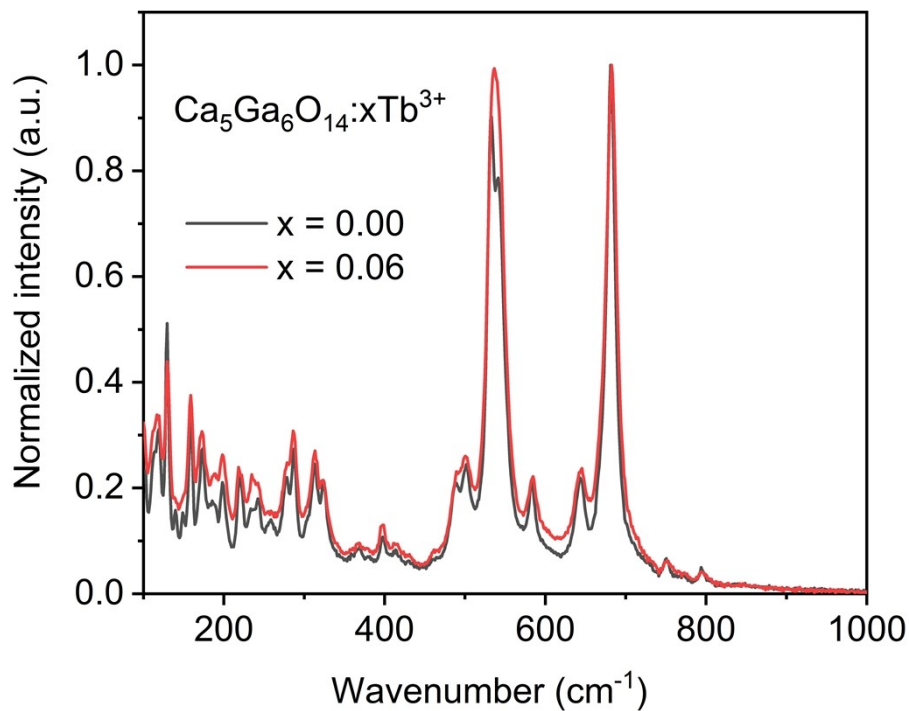


Figure S12. Raman spectra of $\text{Ca}_5\text{Ga}_6\text{O}_{14}:\text{xTb}^{3+}$ ($x = 0.00$ and 0.06) phosphors

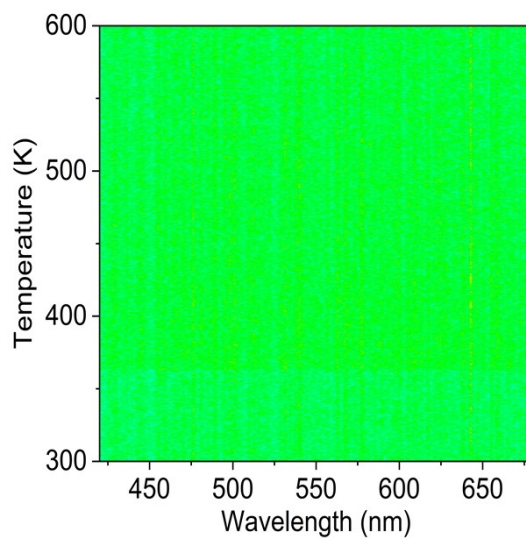


Figure S13. Temperature-wavelength-intensity plot of three-dimensional TL mapping of $\text{Ca}_5\text{Ga}_6\text{O}_{14}:\text{6\%Tb}^{3+}$ phosphor after thermal annealing at 673 K.

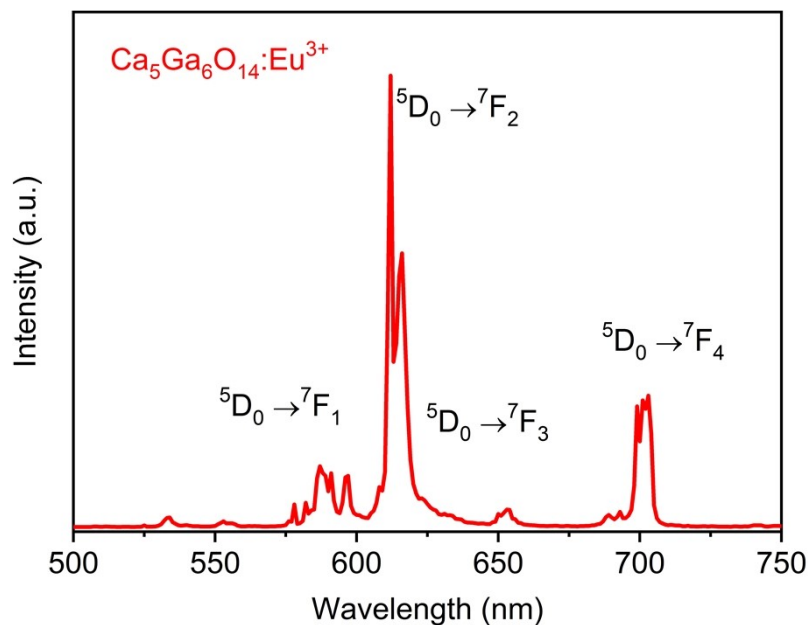


Figure S14. PL spectra of $\text{Ca}_5\text{Ga}_6\text{O}_{14}:\text{Eu}^{3+}$ phosphor under 260 nm UV light excitation

Table S1 EDS analysis on element compositions

Element	Line Type	Apparent Concentration	k Ratio	Wt%	Wt% Sigma	Atomic %
O	K series	6.65	0.02237	51.16	0.26	79.28
Ca	K series	2.32	0.02073	13.37	0.12	8.27
Ga	L series	3.21	0.03007	34.65	0.22	12.32
Tb	L series	0.10	0.00097	0.82	0.30	0.13
Total:				100.00		100.00

Table S2 CIE coordination (x, y) of the $\text{Ca}_5\text{Ga}_6\text{O}_{14}:x\text{Tb}^{3+}$ phosphors with different doping concentrations

Tb^{3+} doping concentrations	CIE-x	CIE-y
0.02	0.328	0.485
0.04	0.339	0.519
0.06	0.338	0.529
0.08	0.342	0.538

Table S3 The reported piezoelectric strain tensor d_{ij} in unite of pm/V

Compound	d_{33}	d_{31}	d_{15}
AlN	5.4	-2.1	-2.9
GaN	2.7	-1.4	-1.8
ϵ -Ga ₂ O ₃	4.85	-0.48	9.622

Table S4 The reported piezoelectric stress tensor e_{ij} in unite of $10^{-10}\text{C}/\text{m}^2$

Compound	e_{33}	e_{31}	e_{15}
AlN	1.61	-0.65	-0.34
ZnO	1.33	-0.65	-0.49
GaN	0.67	-0.37	-0.23
ϵ -Ga ₂ O ₃	0.941	0.011	0.595